HYDRODEOXYGENATION OF GUAIACOL OVER Pt/Ga-MESOPOROUS CATALYSTS

Lorena Rivoira, M. Laura Martínez, Andrea Beltramone

Centro de Investigación en Nanociencia y Nanotecnología (NANOTEC), Facultad Regional Córdoba, Universidad Tecnológica Nacional, Córdoba, Argentina.

**E-mail: lrivoira@frc.utn.edu.ar*

Resumen

La hidrodesoxigenación (HDO) de guayacol, utilizado como molécula modelo, ha sido estudiada en un reactor batch sobre catalizadores de platino soportado sobre SBA-15 a 12 atm de presión y diferentes temperaturas, utilizando dodecano como solvente de reacción. El catalizador fue modificado con galio, incorporándolo como heteroátomo en la red mesoporosa de silíceos, mediante síntesis directa con el objetivo de modificar la naturaleza del soporte, pretendiendo mejorar la actividad catalítica del material. La acidez moderada que genera la incorporación de galio mejora la distribución de las especies activas de platino. En base a los resultados obtenidos el catalizador más activo en la HDO de guaiacol a 12 atm y 200°C fue Pt-Ga-SBA-15, con un 95% de conversión de reactivo en menos de 1 h de reacción.

Palabras clave: hidrodesoxigenación, guayacol, galio, platino, mesoporoso.

Abstract

The hydrodeoxygenation (HDO) of guaiacol as model compound, has been studied in a batch reactor over SBA-15 supported platinum catalysts at 12 atm and different temperatures, using dodecano as solvent reaction. The catalyst was modified with gallium incorporated as heteroatom into the mesoporous siliceous framework by direct synthesis in order to modify the nature of the support pretending to improve the catalytic activity of the material. Mild acidity generated by gallium incorporation enhance the distribution of platinum active species. Pt-Ga-SBA-15 was the most active catalyst in HDO of guaiacol at 12 atm and 200°C. 95% of reactive conversion was obtained in less than 1 h of reaction.

Keywords: hydrodeoxygenation, guaiacol, gallium, platinum, mesoporous.

Estaría dispuesta a someter mi trabajo al volumen especial dedicado al CICAT 2020 en alguna de las revistas internacionales: Catalysis Today o Topics in Catalysis en caso de que los revisores y el comité científico seleccionen mi trabajo.

1. Introduction

Pyrolysis is an old thermochemical transformation that in recent years has captivated scientific community because this is a viable way to convert agricultural and forestry waste in liquid fuels becoming a profitable process.

Lignocellulose is a structural component present in plants and this way it is the most abundant, inexpensive and renewable biomass all over the world [1]. It has three main components: cellulose, hemicellulose and lignin. Bio-oils obtained from lignocellulose by fast pyrolysis often have high oxygen contents (O/C≈) and they are characterized by low heating values, poor stability, high viscosity and corrosiveness [2, 3]. From a chemical point of view lignin-derived compounds are too complex to be used as liquid fuel and require upgrading, either with catalytic hydroprocessing [3-7], zeolite upgrading [3, 5, 8] or aqueous phase processing [6, 8]. Hydrodeoxygenation (HDO) has been proposed as a promising process to enhance the liquid product quality. Hydrotreating occurs in presence of a catalyst upgrading bio-oils to hydrocarbon via oxygen removal. HDO studies usually employ model compounds such as phenol, anisole and guaiacol to simulate bio-oil considering those molecules the most representative because they are in large proportion present in bio-oils derived from lignocellulosic biomass. Guaiacol (2-methoxyphenol) has propensity for coke formation, it is the most difficult to deoxygenate [9] and has two representative oxygenated functional groups (methoxy and phenolic). Many researchers have applied traditional HDS catalysts (sulfided Co-Mo/γ-Al2O3 or Ni-Mo/ γ-Al2O3) for the HDO of guaiacol [3, 10]. However, these industrial hydrotreating catalysts have some disadvantages for HDO of guaiacol because sulfur contamination of products may occur and consequently the catalyst deactivation by surface sulfur stripping [11, 12]. Thereby, non-sulfided catalysts are receiving more attention, transition-metal-based catalysts such as Ni/ZrO2 [13], Ni/SiO2 [14, 15], MoN/Al2O3 and MoN/SBA-15 [13], Fe/SiO2 and Fe/AC [16], Sn/CNF/Inconel [17], V2O5/Al2O3 [18], Ni/W/TiO2 [19] and noble metal catalysts (Pt, Pd, Rh and Ru) supported on activated carbon, siliceous mesoporous material and alumina [20-27].

HDO activity, as well as product selectivity are influenced by the nature of the support [28, 29]. Ghampson et al, 2012 [23] reported that there are clear differences between alumina- and SBA-15-supported catalysts in terms of products distribution. Mo nitride over alumina-supported catalysts produce mostly cathecol, while the SBA-15-supported catalysts produced more phenol. The acidic properties of alumina may be responsible for cathecol formation. The active phase is responsible for de catalytic activity, however, the support modified the nature of the active sites of nitrides and affects the product selectivity. Mesoporous silica materials, such as SBA-15, are interesting as supports in heterogeneous catalysis due to their high specific surface areas, high structure regularity, controllable pore diameter, narrow pore size distribution and large pore volumes.

The incorporation of a metallic heteroatom into a siliceous mesoporous matrix may generate alterations over the support surface. Our previous results [30] indicated that Ga confers weak acidity to the SBA-15 surface in agreement with literature [31]. Mild acidity in the support could improve the activity of the catalyst in HDO of guaiacol because of the interaction between the support and the active species, eluding coke formation. According to literature platinum has high activity and stability for hydrogenation of aromatics at low reaction temperatures and moderate hydrogen pressures [32].

In this work we study the activity of Pt-Ga-SBA-15 catalysts on the HDO of guaiacol and compare its activity with Pt-SBA-15. We evaluate the influence of the support modification with gallium as heteroatom of the siliceous framework.

2. Experimental

3.1. Synthesis of SBA-15

SBA-15 material has been synthesized according to the procedure described by Zhao et al [33]. A solution of template was prepared by dissolving 1.5 g of P123 in 48 mL of HCl 2M (pH = 1). The solution was heating up to 50 °C, and then 3.7 mL (0.016 mol) of tetraethylorthosilicate (TEOS) were added dropwise under vigorous stirring. The mixture was held statically at constant temperature. After 24 h, temperature was set at 80 °C and maintained for 48 h. The solid obtained was then filtered and washed repeatedly with distilled water. Next, the material recovered was washed with a water/ethanol mixture for 2 h. Again, the material was filtered, washed and placed into an oven for drying at 100°C. The material as synthesized was calcined at 500°C for 5 h. Molar ratios of the synthesis were 1TEOS: 158 H2O: 6HCl: 1.6x10-2 P123.

3.1. Synthesis of Ga-SBA-15

In order to modify the acidic characteristics of the support, Ga was incorporated in the matrix of SBA-15 using the following technique: post-synthesis gallium incorporation. An aqueous solution of Ga(NO3)3 was used as gallium source. The gallium concentration was calculated in order to obtain samples with Si/Ga ratio of 20. SBA-15 (1 g) material was mixed with 50 mL of the gallium solution at room temperature for 20 h. The sample was then filtered and washed with distilled water and dried at 60 °C overnight, to be finally calcined in air at 500 °C for 5 h. The material obtained was denoted as Ga-SBA-15.

3.1. Synthesis of Pt-SBA-15 and Pt-Ga-SBA-15

Platinum (Pt) nanoparticles were incorporated into SBA-15 support or Ga-SBA-15 by wet impregnation method. Chloroplatinic acid was used as metal precursor (H2PtCl6xH2O)). It was dissolved in 50 mL of ethanol at 50°C under reflux, to have a nominal content of 0.5wt.% of Pt in the final solid. A finely ground powder fraction of the corresponding support was dried in static air at 120°C for 12 h, then, it was directly incorporated to the platinum solution. It was placed in a rotary evaporator to remove excess of ethanol at about 50°C and 60 rpm. The obtained powder was then dried at 120°C overnight, and desorbed at inert atmosphere (nitrogen flow of 20 mL/min) from 25°C to 470°C with a slope of 4°C/min and kept at 470°C during 5 h. Then the samples were calcined at 500°C for 5 h. The sample was finelly reduced in H2 flow of 20 mL/min at 470°C.

3.1. Characterization of the catalysts

XRD patterns were collected by using a continuous scan mode. The scan speed was 0.02 deg (2 θ)/min in the Philips X'Pert PRO PANalytical diffractometer, operating with CuKα X-ray radiation (X-ray generator current and voltage set at 40 mA and 45 kV), using small divergence and scattering slits of 1/32 mm and a goniometer speed of 1.2º (2θ) min-1. The scanning range was set between 0.5º and 5º. The sample was crushed previously and placed in an aluminum sample holder. Elemental analysis was performed by inductively coupled plasma-atomic emission spectroscopy (VISTA-MPX) operated with high frequency emission power of 1.5 kW and plasma airflow of 12.0 L/min. TPR was performed using a Micromeritics Chemisorb 2720 apparatus, with a flow of 14 mL/min of 10 mol% of H2/N2 heating up to 500 ºC, with a preheating treatment at 380 °C in an inert atmosphere (N2). N2 adsorption/desorption isotherms at -196°C were measured on ASAP 2020 equipment after degassing the samples at 400°C. The pore size distribution of the samples was determined by the Nonlocal Density Functional Theory (NLDFT) applied for cylindrical pores of siliceous adsorbents at -196°C, using the adsorption branch. The same models were applied to calculate mesopore volumes; the specific surface area was determined by Brunauer-Emmett-Teller (BET) method.

TEM were recorded in a JEOL 2100F microscope operated with an accelerating voltage of 200 kV (point resolution of 0.19 nm); coupled with energy-dispersive X-ray spectroscopy (EDS).

3.1. Catalytic Activity

The catalytic activity was measured in a 4563Parr reactor at 12 atm of hydrogen and 360 rpm at different temperatures. Feed consisted in 50 mL of guaiacol (99 % SIGMA-ALDRICH) in dodecane, the amount of catalyst was set according to the ratio of guaiacol mass /catalyst mass=2.5. The guaiacol conversion was analyzed with a HP 5890 Series II GC and HP-5 column.

3. Results and discussion

3.1. Characterization of the catalysts

3.1.1.XRD

As illustrated in Fig. 1, the Ga-SBA-15 sample exhibits a low-angle XRD pattern typical of ordered mesoporous solids with an intense peak at $2\theta \sim 0.85°$ corresponding to the (1 0 0) reflection, as well as minor peaks at $2\theta \sim 1.45$ and 1.68° arising from (1 1 0) and (2 0 0) planes. For the Pt-Ga-SBA-15 sample, those peaks are less intense. The reflection of the (1 0 0) plane is clearly observed. This fact can be assigned to the distortion in the hexagonal mesopore array caused by the Pt incorporation, leading to a material with lower mesoscopic order [34, 35].

In this way, the inset in Fig. 1 displays the high-angle XRD patterns of the all samples, the Pt-containing materials show a broad bottom reflection centered at 23°, proper of the amorphous nature of Pt-SBA-15 pore walls. Characteristic peaks of Pt clusters or Pt-oxides are not shown in the diffraction patterns. We can conclude that the incorporation of gallium as a heteroatom into the silicon framework favors a better dispersion of platinum.

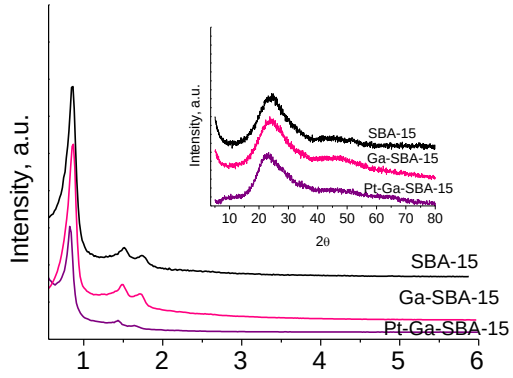

Figure 1. XRD pattern of the synthesized samples

3.1.2. TEM

The morphology of the support wiyh metallic nanoparticles over the synthetized samples were examined by means of transmission electron microscopy (TEM). The TEM images of the catalysts are shown in Figure 2. The sample showing the well-ordered 2D-hexagonal pore arrangement (p6mm) typical of SBA-15 materials. A segregated phase or non-framework species was not observed on the images, indicating that gallium was homogenously dispersed over the SBA-15 framework. The images show that pore-structures of the Ga-SBA-15 materials were intact after Pt impregnation. They also show that some Pt condensed into nanometer-size particles on the Ga-SBA-15 surface. The sample with Pt presented high dispersion of metal particles.

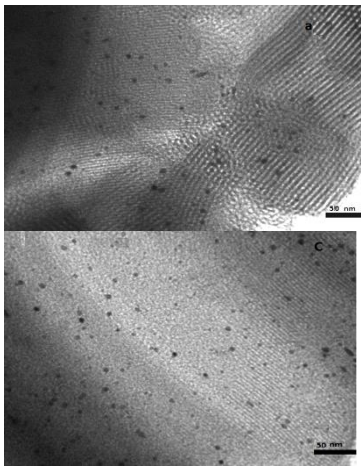

Figure 2. TEM images of Pt-Ga-SBA-15

The textural and structural properties of Pt catalysts supported on SBA-15 and Ga-SBA-15 are given in Table 1. Pt cluster was not observed in the samples, showing high dispersion determined by TEM. The incorporation of a metal in the structure therefore leads to a slight decrease in the surface area but the pore diameter and the mesoporous character are maintained.

Table 1. Physicochemical and structural properties of the catalysts.

Material	A (m^2/g)	V_p (cm^3/g)	D_p (nm)
SBA-15	1080	1.31	8.20
Pt-SBA-15	690	1.10	7.95
Pt-Ga-SBA-15	670	0.97	7.83

V_P: Total pore volume; A: BET surface area; D_P: Pore diameter determined by NLDFT method from the adsorption branch

3.1.3. Catalytic activity

In the present work, we evaluated guaiacol conversion over Pt-based catalysts and compared the catalytic properties of platinum over SBA-15 and Ga-SBA-15. As shown in Fig. 3, the catalyst modified with gallium was more active than without it, maintaining this tendency at three different temperatures. It has been reported that gallium incorporation into the support modified the nature of the SBA-15 surface conferring weak acidic properties to the catalyst [31].

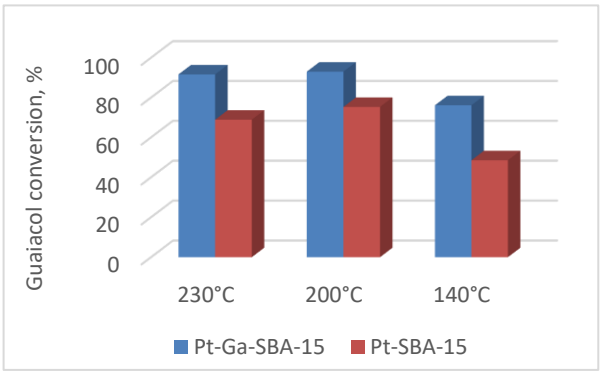

Figure 3. Catalytic activity of Pt-Ga-SBA-15 and Pt-SBA-15 at 12 atm and 230°C, 200°C and 140°C. Mass ratio G/cat=2.5 (360 rpm) Reaction time: 7 h.

The interaction between platinum active species and the surface is possibly modified because of the presence of Bronsted and Lewis acidity, resulting in a better catalytic activity. In order to prove that platinum is the active species that allows the reaction occurs, a blank reaction using Ga-SBA-15 was carried out obtaining less than 15% wt. of guaiacol conversion.

Fig. 4 a) and b) shows the evolution of guaiacol during the HDO. The guaiacol conversions were calculated from the initial reagent in the reactor feed and the residuary guaiacol recovered in the

samples taken at various times.

The experiments using Pt-SBA-15 reached the highest conversions after 4 h of reaction with a maximum of 75% wt., whilst Pt-Ga-SBA-15 displayed 95% wt. of guaiacol conversion after only 1 h of reaction. It was observed that there is an effect of temperature over the catalytic activity for both materials. Temperatures used were 140, 200 and 230°C without altering other conditions. Figure 4 a) and b) shows that the reaction rates obtained with gallium modified support were higher at every temperature. It was found that when temperature rises 240°C could be a coke formation. A middle temperature of 200°C resulted to be the most efficient for HDO of guaiacol at 12 atm. The most active catalyst was Pt-Ga-SBA-15 at 200°C of reaction temperature.

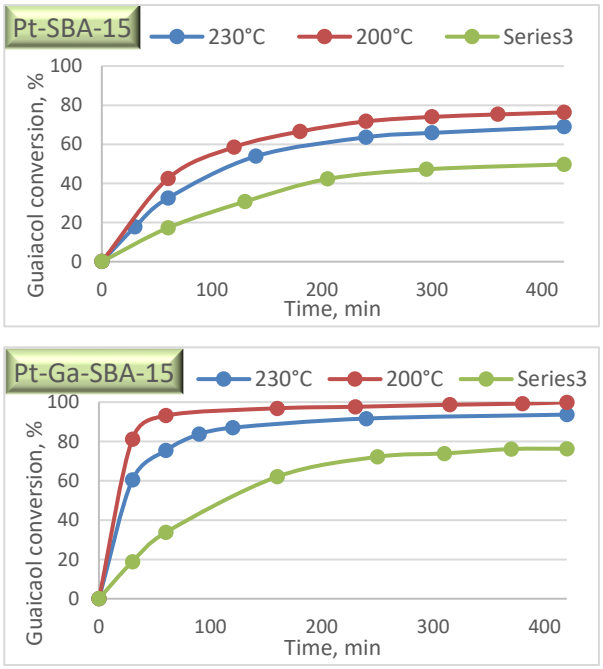

Figure 4. a) Catalytic activity for Pt-SBA-15 and for b) Pt-SBA-15 under constant reaction conditions.

A large number of products were found, mainly phenol, catechol and cyclohexane.

4. Conclusions

We have prepared SBA-15 and Ga-SBA-15 supported platinum catalysts and analysed their activity in HDO in terms of guaiacol conversion and temperature effects at constant hydrogen pressure. Wet impregnation method was used for platinum incorporation. Gallium incorporation as heteroatom into the siliceous support improved Pt nanoparticles dispersion, as we could see in Fig. 2 because Ga generate weak acidity over the surface of SBA-15 conferring to the catalyst new properties. It was confirm that platinum active sites can be enhanced by modification of the support nature. The results showed that 95% wt. of guaiacol conversion is reached in a very short reaction time (1 h) at 12 atm and 200°C using Pt-Ga-SBA-15 with 0.5% wt. of platinum loading.

5. Acknowledgments

María L. Martínez and Andrea Beltramone. NANOTEC, CONICET, National Technology University, Cordoba Faculty, Maestro Lopez y Cruz Roja Argentine. We acknowledge the financial support of CONICET Argentina, PIP CONICET 11220120100218CO. 2014 -2017.

6. References

[1] C.-H. Zhou, X. Xia, C.-X. Lin, D.-S. Tong, J. Beltramini, *Chem. Soc. Rev.*, 40 (2011) 5588.
[2] S. Czernik, A.V. Bridgwater, *Energy Fuels*, 18 (2004) 590.
[3] H. Wang, J. Male, Y. Wang, *ACS Catal.*, 3 (2013) 1047.
[4] D.M. Alonso, S.G. Wettstein, J.A. Dumesic, *Chem. Soc. Rev.*, 41 (2012) 8075.
[5] G.W. Huber, J.A. Dumesic, *Catal. Today*, 111 (2006) 119.
(6) J.C. Serrano-Ruiz, J.A. Dumesic, *Energy Environ. Sci.*, 4 (2011) 83.
(7) D.C. Elliott, *Energy Fuels*, 21 (2007) 1792.
[8] T.P. Vispute, G.W. Huber, *Green Chem.*, 11 (2009) 1433.
(9) E. Furimsky, *Appl. Catal. A*, 199 (2000) 147-190.
(10) Q. Bu, H. Lei, A.H. Zacher, L. Wang, S. Ren, J. Liang, Y. Wei, Y. Liu, J. Tang, Q.Zhang, R. Ruan, *Bioresour. Technol.*, 124 (2012) 470.
(11) O.I. Senol, E.M. Ryymin, T.R. Viljava, A.O.I. Krause, *J. Mol. Catal. A: Chem.*, 277 (2007) 107–112.
(12) A.V. Bridgwater, *Appl. Catal. A: Gen.*, 116 (1994) 5–47.
(13) C.M. Pichler, D. Gu, H. Joshi, F. Schüth, *J. of Catal.*, 365 (2018) 367-375
(14) M.V. Bykova, D.Y. Ermakov, V.V. Kaichev, O.A. Bulavchenko, A.A. Saraev, M.Y. Lebedev, V.A. Yakovlev, *Appl. Catal. B: Environ.*, 113–114 (2012) 296–307.
(15) S.-K. Wu, P.-C. Lai, Y.-C. Lin, *Catal. Lett.*, 144 (2014) 878–889.
(16) R.Olcese, M.M. Bettahar, B. Malaman J. Ghanbaja, L. Tibavizco, D. Petitjean, A. Dufour, *Appl. Catal. B: Environ.*, 129 (2013) 528-538.
(17) M.A. González-Borja, D.E. Resasco, *Energy Fuels*, 25 (2011) 4155–4162.

(18) J. Filley, C. Roth, *J. Mol. Catal. A:Chem.*, 139 (1999) 245–252.
(19) Y.-K. Hong, D.-W. Lee, H.-J. Eom, K.-Y. Lee, *Molecular Catalysis*, 392 (2014) 241–246
(20) D. Gao, C. Schweitzer, H.T. Hwang, A. Varma, *Ind. Eng. Chem. Res.*, 53 (2014) 18658–18667.
(21) M. Hu, X. Wang, *Catal. Today*, 263 (2016) 98–104.
(22) Q. Lai, C. Zhang, J.H. Holles, *Appl. Catal. A: Gen.*, 528 (2016) 1–13
(23) I.T. Ghampson, C. Sepúlveda, R. Garcia, J.L. García Fierro, N. Escalona, W.J. DeSisto, *Appl. Catal. A: Gen.*, 435– 436 (2012) 51– 60.
(24) Z. He. M. Hu, X. Wang, *Catal. Today*, 302 (2018) 136-145.
(25) A. Gutierrez, R.K. Kaila, M.L. Honkela, R. Slioor, A.O.I. Krause, *Catal. Today*, 147 (2009) 239‑246.
(26) T. Nimmanwudipong, R.C. Runnebaum, D.E. Block, B.C. Gates, *Energy&Fuels.*, 25 (2011) 3417–3427.
(27) Y.-K. Hong, D.-W. Lee, H.-J. Eom, K.-Y. Lee, *Appl. Catal. B: Environ.*, 150– 151 (2014) 438– 445.
(28) A. Centeno, E. Laurent, B. Delmon, *J. Catal.* 154 (1995) 288‑298.
(29) V.N. Bui, D. Laurenti, P. Delichère, C. Geantet, *Appl. Catal. B: Environ.*, 101 (2011) 246‑255.
(30) L. Rivoira, M.L. Martínez, O. Anunziata, A. Beltramone. *Micropor. Mesopor. Mater.*, 254 (2017) 96-113
(31) M.J. Gracia, E. Losada, R. Luque, J.M. Campe1lo, D. Luna, J.M. Marinas, A.A. Romero, *Appl. Catal.* A: Gen., 349 (2008) 1489155.
(32) S.A.K. Kumar, M. John, S.M. Pai, Y. Niwate, B.L. Newalkar, *Fuel Process. Technol.*, 128 (2014) 303.
(33) D. Zhao, J. Feng, Q. Huo, N. Melosh, G. Fredrickson, B. Chmelka, G. Stucky. *Science*, 279 (1998) 548.
[34] C. Liu, R. Tan, N. Yu, D. Yin, *Micropor. Mesopor. Mater.*, 131 (2010) 162.
[35] J.M. Juárez, M.B. Gómez Costa, O.A. Anunziata, *Internat. J. Energy Res.*, 39 (2015) 128.